DOI: 10.21203/rs.3.rs-3627549/v1

Prediction of rolling contact fatigue loci: a comparison between dynamic and a simplified quasi-static approaches

P. A.P. Pacheco
Federal Institute of the Southeast of MG
P. G. Ramos
Universidade Estadual de Campinas
T. L. Sá
Polytechnic School University of São Paulo
G. F.M. Santos
Federal University of Espírito Santo
A. Gay Neto
Polytechnic School University of São Paulo
A. A. Santos
aute@fem.unicamp.br

Universidade Estadual de Campinas

Research Article

Keywords: Pummeling, Wheel/rail contact, Multibody simulation, Contact

Posted Date: November 21st, 2023

DOI: https://doi.org/10.21203/rs.3.rs-3627549/v1

Additional Declarations: No competing interests reported.

Version of Record: A version of this preprint was published at Multibody System Dynamics on April 8th, 2024. See the published version at https://doi.org/10.1007/s11044-024-09979-z.

Abstract

Predicting fatigue and wear on wheels and rails is a key to find ways to improve the service life of a railway track and the rolling stock. Rails experience contact with a range of wheel profiles that will pummel their surface at different positions with different intensities. This work compares two methods for evaluating pummelling analyses for the wheel-rail interaction: simplified quasi-static model and multibody dynamics simulations. The first one is solved using the GIRAFFE program and simulates the interaction of a single wheelset with the rail in a quasi-static approach. The second one evaluates the full dynamics of a railway wagon on a track layout using multibody dynamics simulation programs SIMPACK® and VAMPIRE®. The proposal of a quasi-static model is to reduce the time and computational effort to perform a pummelling analysis and quickly evaluate thousands of cases of wheel-rail contact. Track parameters and vehicle loads of a heavy haul railway are considered for the simulations. The results showed that the quasi-static model has a good correlation with the dynamic models on tangent track sections. For the curved sections, differences were observed in the distribution of pressures due to the absence of creep forces in the quasi-static model. The comparison between the models also showed slight distinct results due to the difference in how the contact is calculated in each approach. The quasi-static approach reduced the time consuming by at least 73.4% over the multibody approach. Notwithstanding, the proposed model shows to be promising on replacing complete dynamic analysis for time consuming tasks as pummelling.

1 INTRODUCTION

The prediction of fatigue and wear on wheels and rails is crucial to improve the service life of a railway track and the rolling stock. Thus, it is necessary to accurately determine the wheel/rail contact loci and stress [1]. In practice, rails experience contacts with a range of different wheel profiles that will pummel the rail surface at different positions, with different intensities. A pummelling analysis aims to understand the accumulated effect of a large population of wheelsets. This concept was first introduced by Magel and Kalousek [2]. The authors define it as the process of managing the position, severity, and frequency of contacts on the surfaces of the wheels and rails to reduce the increments of wear and fatigue. In the context of rail profile simulation and design, pummelling can be employed in the analysis of a track section subjected to the transit of a wide variety of real wheel profiles obtained from the measurement in the consist for that operation or scenario.

One of the main steps of pummelling is contact analysis. Through the literature review, one can find several methods to calculate the wheel/rail (W/R) contact. Among them are analytical methods, numerical ones, and online and offline approaches. The application of numerical methods for W/R contact calculation has become of great importance for railway applications in recent years [3], especially to be used in multibody dynamics simulations.

The multibody dynamics solvers can run online or offline. In the online way, the contact is calculated using an iterative process at each time step, while offline approaches use interpolation values from look-

up tables (LUT), pre-calculated. The online way presents better accuracy while the offline is faster.

Pombo and Ambrósio [4] proposed a generic formulation to determine the contact forces at the wheel–rail interface during dynamic analysis. With this model, the wheel-rail contact points' coordinates are calculated online at every time-step, using an interpenetration strategy. Normal contact forces are computed using Hertz contact theory. With creepages and normal contact forces known, at least three distinct approaches can be used to calculate creep forces: Kalker linear theory; Heuristic nonlinear force model; and Polach formulation. Meli and Ridolfi [5] presented an online contact model that incorporates degraded adhesion conditions, suitable for wheel-rail contact applications that involve multiple bodies. Normal forces are calculated with the aid of global Hertz theory. Using the new adhesion model, the tangential contact forces and adhesion coefficient are calculated. A comparison between the online Knife-edge Equivalent Contact (KEC) constraint and offline look-up table (LUT) methods is presented by Yu et al. [6]. In the implementation of the LUT method, a penetration-based elastic contact model is applied to the flanges and a constraint-based formulation is applied to the treads of the wheels. Based on Hertz's contact theory, normal contact forces are defined in terms of stiffness and damping ratio. As a result, large magnitude values for stiffness parameters are generated and that will affect computational efficiency and numerical stability. Using the KEC method, where an infinitely narrow rail contacts an equivalent wheel, tread-flange transitions are regularized to account for tread and flange contacts, simultaneously. Lagrange multipliers are used to determine normal contact forces, thereby avoiding numerical disadvantages related to stability in the case of high contact stiffness values. Although there is good agreement in the kinematic results between the two methods, the KEC method was up to 20% more efficient than the LUT method.

The pummelling approach is a helpful tool to evaluate W/R performance, but it is computationally expensive [7], as it requires the execution of a large volume of analyses. Therefore, it is important to use simplified and reliable models to represent the wagon dynamics.

On a multibody dynamic simulation of a complete wagon (Fig. 1), regions of transient dynamics can be observed, entering and exiting a curve. There are also regions of steady-state positions, where the wagon is on dynamic equilibrium with no time-varying wheelset lateral positions, which means a quasi-static equilibrium (considering inertial effects). So, instead of carrying out several full dynamic simulations just to obtain their steady-state positions and contact forces on the rails to perform a single pummelling analysis, directly solve the steady-state scenario seems to be more reasonable.

Therefore, unlike the usual approaches that use multibody simulation programs for transient dynamic analysis of the complete interaction between wagon and railway track, Higa, Kina and Gay Neto [8] used a quasi-static model to obtain the steady-state response for the interaction of a single wheelset with a specific section of the railway track. In other words, using a simplified dynamic simulation, it is sought to obtain the equilibrium position of static and dynamic forces. In this way, the assumption is that the quasi-static simulation can represent a steady-state solution, which can be obtained using a full transient dynamic approach, as commonly performed in multibody software environments.

This work evaluates the capabilities of the simplified simulation methodology presented by Higa et al. [8] to generate pummelling analysis in comparison with the results obtained through multibody dynamics simulations carried out in SIMPACK® and VAMPIRE®. Considering track parameters and vehicle loads of a heavy haul railway in Brazil, these simulations are computed to obtain the accumulated contact pressure for new and worn rails subjected to the traffic of a family of wheels with different geometric profiles.

The goal is to compare the different approaches and software in predicting contact pressure and position to a variety of wheel and rail profiles. The sum of a set of pressure distributions will give an indication on the regions of the rail that are more likely to experience rolling contact fatigue (RCF) [2]. If the quasi-static model shows to be reliable, the approach can be used to easily and quickly design rail profiles to last longer.

2 METHODS

In this section, the dynamic and quasi-static models are presented for the pummeling analysis approach. More specifically, the section is organized as follows: the dynamics models of the wagon using the commercial software SIMPACK® and VAMPIRE® are given in Sec. (2.1). In Sec. (2.2) we discuss the quasi-static model employed by the software GIRAFFE. Finally, in Sec. (2.3) the pummeling analysis for the case of a heavy-haul railway in Brazil is presented.

Dynamic simulations

The heavy haul wagon GDE-Ride Control was modeled in SIMPACK® and VAMPIRE®. It is a meter gauge three-piece bogie wagon with 27.5 tons per axel, employed for ore transportation in a Brazilian railway. The model of the wagon was validated by comparison with previous results from NUCARS® and experiments performed under supervision of the ore transportation company. Figure 2 shows the comparison of the results from the three software for a specific sector of the railway.

The primary suspension includes a shear pad between the wheelset bearing and the side frame pedestal. The pad adapter is made of an elastomeric material positioned between two steel plates [9]. It was modeled in SIMPACK® using three springs between the wheel axle and the side frame. The inner and outer springs feature a vertical stiffness and a vertical damping parameter (z). The central spring has stiffness and damping in the longitudinal (x), lateral (y), and rotational (yaw -about z) directions. The magnitudes of stiffness and damping adopted include the influence of the pad. In VAMPIRE®, the primary suspension is defined by bushing elements, that have linear stiffness and damping, and non-linear stiffness elements. These elements together represent pitch and yaw stiffness and vertical, roll and yaw damping.

The secondary suspension is modeled in SIMPACK® with bushing springs. The spring system is composed of four springs arranged in a square distribution, with a vertical stiffness and a vertical damping parameter (z). A fifth spring is in the center, which has stiffness properties and damping

parameters in all directions. In the same suspension system, the wedges with constant damping were modeled using discrete contact elements and considering dry friction between the contact surfaces. In VAMPIRE®, the secondary suspension is modeled as a seven-spring package with vertical, lateral and longitudinal linear stiffness and a central element of non-linear vertical stiffness. The wedge is represented by two elements of lateral non-linear stiffness, four friction elements and a spring with longitudinal linear stiffness.

The connection points between the wagon box and the bogies are modeled on the center plate and the roller side bearing. In SIMPACK®, dry friction elements were adopted on the side of the center plate for tangential contact and universal point contact elements for the vertical direction. For the contact model of the roller side bearing, a spring (bushing type) was used with the vertical stiffness of contact with a gap, since the type of balance support modeled is not of constant contact, like the one adopted for modeling the primary suspension. In VAMPIRE® the center plate is modeled by four damping elements and twelve friction elements at the ends of the plate, in addition to four non-linear stiffness elements at the same points. In the plate's center, there are two other non-linear rigidity elements, longitudinal and lateral. The roller side bearing is represented by a non-linear vertical stiffness element with a gap of 8 mm.

As already mentioned, the loaded axle weight for this GDE wagon is 27.5 tonnes. Because of that weight, the wagon is considered a heavy-haul freight car. The models of the bogies for this wagon on SIMPACK® and VAMPIRE® are shown in Fig. 3 and Fig. 4, respectively.

The wheel-rail contact forces in SIMPACK® and VAMPIRE® are calculated from a simplified Kalker's theory, which defines the relationship between the creepages and the creep forces. The Kalker's linear theory (Eq. 1) uses the well-known Kalker coefficients (C_{ij}) to determine the relationship between creepages and creep forces and moments. In this case, the longitudinal and lateral forces are given by a linear function [10],

$$\begin{bmatrix} F_x \\ F_y \\ M_z \end{bmatrix} = -Gab \begin{bmatrix} C_{11} & 0 & 0 \\ 0 & C_{22} & \sqrt{ab}C_{23} \\ 0 & -\sqrt{ab}C_{23} & abC_{33} \end{bmatrix} \begin{bmatrix} \xi_x \\ \xi_y \\ \phi \end{bmatrix}$$

1

.

F_x, F_y and M_z are the longitudinal creep force, lateral creep force and spin creep moment. C_{ij} (i,j = 1,2 and 3) are constants that depend on the Poisson coefficient v and the ratio of the semi-axes of the contact ellipse patch. G is the modulus of rigidity, while a and b are the major and minor semi-axis of the contact ellipse, respectively. ξ_x, ξ_x and φ are the longitudinal creep, lateral creepages, and spin creepage. The full Kalker's theory is implemented in the CONTACT software (software that numerically solves normal and tangential contact problems).

Normal and tangential W/R contact forces for the contact points are calculated using FASTSIM in SIMPACK®. It is a very fast method for calculating creep forces, widely used in contact W/R programs [11]. FASTSIM is a simplified approach based on that proposed by Kalker [12], in which the surface displacements are linearly related to the surface traction (Eq. 2) [13],

$$u = Lp$$

2

,

where *p* is the local tension and *L* is the flexibility constant, which is derived from the linear theory constants (Eq. 1).

For FASTSIM, Kalker proposed that *L* = *Lx*, *Ly* e *Lφ*. Thus, the flexibility constant is given by [14]:

$$L = \frac{\left(|\xi_x| L_x + |\xi_y| L_y + c|\xi_\phi| L_\phi\right)}{\left(\xi_x^2 + \xi_y^2 + c\xi_\phi^2\right)}$$

3

$$L_x = \frac{8a}{3C_{11}G}, L_y = \frac{8a}{3C_{22}G}, L_\phi = \frac{\pi a\sqrt{a/b}}{4C_{23}G}, c = \sqrt{ab}$$

4

In SIMPACK®, the FASTSIM algorithm assumes an elliptical contact patch and discretizes it into a grid of m_x x m_y elements (Fig. 5) [15]. Tangential forces are determined by integrating tangential stresses in grid elements numerically. Tangential stresses accumulate from the contact patch's front boundary until the local saturation limit is reached. Grid discretization in longitudinal direction is constant. The grid is automatically refined in the lateral direction around the spin pole if the pole lies within the contact patch. According to the contact patch width, the boundary indicates the minimum allowed grid width. It is determined from the initial discretization by $m_y = m_x$: $t = 1/[5(my - 1)]$. SIMPACK suggest $t = 0.02$ for $m_y = 11$ as default, which is Kalker's recommendation [12, 16].

VAMPIRE® uses Hertzian contact theory to determine the normal forces and an off-line look-up table (LUT) to calculate the tangential contact forces. The use of LUT in the W/R contact requires a pre-calculated table that stores the values of the function determined with the CONTACT software, such as the normal and creep forces, in a set of points that constitute the domain of the table. Then, during a simulation, for a given input such as the relative position and orientation between rail and wheel, the output parameters required for the dynamic analysis are computed through the interpolation of data from the LUT. Thus, the online calculation of a cumbersome function, which is generally slow but accurate, can be promptly approximated through the linear interpolation of tabulated data [17].

VAMPIRE creates a multidimensional look-up table from the cross-sectional profiles of the wheels and rails using the Contact Data Generation preprocessor [18]. The program calculates the lateral displacement of each wheel relative to the rail at each time step. Based on this value, the contact data for each patch between wheel and rail will be looked up. The creepages for each wheel-rail contact patch are calculated using the position, rolling radius, and contact angle obtained for each contact patch as follows.

$$\xi_x = 1 \mp \frac{\dot{W} r_{\pm} \dot{P} l_R + \dot{X}}{V} \tag{5}$$

$$\xi_y = \left(\frac{r_{\pm} \dot{P} - \dot{W}}{V} \right) \sec(\delta) \tag{6}$$

$$\phi = \mp \left(\frac{r_{\pm}}{V} \right) \sin(\delta) + \left(\frac{\dot{W}}{V} \right) \cos(\delta) \tag{7}$$

In equations (5), (6) and (7), *V* is the vehicle speed; *X,Y,W,P* are longitudinal, lateral, yaw and pitch displacements of the wheelset in track axes, respectively; *r* are rolling radii of wheels; *R* is the curve radius of the track; *l* are the distances from the center of the wheelset to the left and right contact patch and δ is the contact angle.

Calculated creepages are then converted to non-dimensional values and used to interpolate non-dimensional creep forces from the Kalker look-up table. Vampire's default Kalker table is based on dry, uncontaminated wheel-rail contact conditions. In the run file, one can modify the coefficient of friction and Kalker factors to approximate other wheel rail contact conditions. As a result, non-dimensional creep forces are converted to actual creep forces at each point of contact between the rail and the wheel [18].

Quasi-static model

Higa et al. [8] proposed a simple 2D model to obtain the wheelset's steady-state lateral position on a given track scenario, instead of solving a multibody transient dynamic simulation of the complete wagon traveling on a track. The model evaluates the normal contact interaction of a single wheelset with a single track section, with a fixed angle of attack for the wheelset. For each wheel/rail pair, the model can deal with multiple pointwise contacts. Its simplification premise is that the wheelset's lateral steady state is governed by the quasi-static equilibrium between gravitational and centrifugal forces (active forces) and normal contact forces on the wheel/rail pairs (reactive forces), as shown in Fig. 6.

In this model the track is fixed, and the wheelset is free to move on the track's transversal plane. Hence, the wheelset has three degrees of freedom, u_x (lateral), u_y (vertical) and ϕ (rotation around longitudinal axis), and its position is given by the vector $\backslash \mathrm{varvec}d$.

$$\varvec{d} = \begin{bmatrix} u_x \\ u_y \\ \phi \end{bmatrix}$$

8

The track is composed of two rails positioned according to the rail cant angle, track gauge and superelevation. The wheelset is comprised of two wheels rigidly linked together and spaced by the back-to-back gauge. Both rails and wheels are modeled as rigid contact surfaces constructed respectively by extrusion and revolution of planar curves, meaning from the rails and wheels profiles.

For a tangent track scenario, only the gravitational load representing the entire wagon weight is applied. For a curved track, it is also applied the centrifugal inertial force dependent of the wagon mass, travel speed and curve radius. Since the model considers a single wheelset, the loads applied are divided proportionally to the number of wheelsets, four for the freight wagon studied here. To capture any effect of lateral load transfer between wheels, the loads are applied not at the center of the wheelset but at a node rigidly attached to the wheelset at a height equivalent to the entire wagon center of mass.

The model solution comprises the wheelset position, which gives the normal contact forces on each wheel/rail pair that will balance the applied loads. To obtain these contact points and normal forces, the model uses the master-master contact formulation [19], a penetration-based (soft contact) approach that can handle multiple contact points. Since the problem of finding multiple contact points and its normal forces is highly nonlinear, the model is solved adopting a dynamic relaxation procedure in which the nonlinear equations are integrated over time using Newmark implicit numerical integration to find the desirable equilibrium solution. The wheelset starts at a position above the rails; the loads are gradually applied; the wheels contact the rails giving a first solution for the normal contact forces; then the wheelset moves laterally seeking its equilibrium position automatically.

On the general 3D master-master contact formulation [19], both surfaces in imminent contact are treated as continuous surfaces with no discretization to pre-defined points; that means there is not a slave surface, as usual in node-surface formulations. The surfaces (Γ_A e Γ_B) are parametrized by their own convective coordinates (ζ, θ) and the contact is assumed to occur on a single point on each surface, consistent to convex surfaces in contact. The pair of contact points is obtained by finding the minimum distance between these surfaces. For that, these points must satisfy the orthogonality conditions given by

$$\varvec{r} = \begin{bmatrix} \Gamma_{A,\zeta_A} \bullet \varvec{g} \\ \Gamma_{A,\theta_A} \bullet \varvec{g} \\ \Gamma_{A,\zeta_B} \bullet \varvec{g} \\ \Gamma_{A,\theta_B} \bullet \varvec{g} \end{bmatrix} = \begin{bmatrix} 0 \\ 0 \\ 0 \\ 0 \end{bmatrix}$$

9

,

where comma "," describes a partial derivative and $\backslash \mathbf{varvec}g = (\Gamma_A - \Gamma_B)$ is the gap function between the surfaces. It is worth noting that the gap function is dependent on the convective coordinates of each surface, but also on the surfaces' vector position.

This set of nonlinear equations, the Local Contact Problem (LCP), is then solved by applying the Newton-Raphson Method or an optimization method. If penetration is verified, a pair of contact normal forces is imposed by a penalty method or a Lagrange multiplier. For more complex surfaces including concave regions, the best approach is to divide the surface into smaller convex surfaces as possible. Then the process consists of applying the same method on each surfaces pairs candidate to contact. A global search procedure can be used to first find which pairs are plausible to contact.

However, the model described in [8] takes advantage of a particular solution of this problem. Since the wheels are idealized as revolution surfaces and the rails as extrusion surfaces, one could restrict the analysis to the transversal plane of the track, and so to the contact between the 2D geometric profiles instead of the 3D complete surfaces, fixing one convective coordinate of each surface. Furthermore, if the geometric profiles are described by a set of circular arcs (Fig. 7), the LCP has an analytical solution, substantially reducing the problem's complexity. This solution is based on the fact that the minimum distance between two circular arcs always occurs on the segment linking their centers. This distance can be easily calculated by the difference between the arc centers distance and the sum of arc radii.

Since this work analyzes the interaction of real wheelsets and tracks, the wheels and rails profiles are obtained by measurement instruments like MiniProf©, which provides a list of almost equidistant points describing the geometric profile. To transform these measurements into a set of tangent circular arcs (arc spline), Silva and Gay Neto [20] developed a fitting procedure that defines arcs based on a curvature function estimated from the points and a least-square optimization to fulfill the geometric and tolerance requirements. Thus, the two 2D geometric profiles on each wheel/rail pair are divided in multiple arcs candidates to contact. Then, multiple contact points can be obtained from the penetration among pairs of arcs, located on wheel and rail sides.

Despite this simplification, the model is still nonlinear due to the multiple contact points detection. The model using the dynamic relaxation method previously described is solved using the software GIRAFFE (*Generic Interface Readily Accessible for Finite Elements*) [21]. Then the results are post processed using the Hertz Contact Theory [22] to obtain the contact ellipse and pressure distribution, using as input the radii obtained by the arc spline fitting procedure.

Pummeling analysis

A pummelling analysis represents the accumulated effect of a set of consecutive contacts, such as profile wear or rolling contact fatigue. The pummelling analyses in this work are presented in terms of

accumulated contact pressure. That is considered an indicator of the occurrence of rolling contact fatigue. Each pummelling analysis shows a graph of the summation of all individual contact pressure distributions over the rail profile. To plot this graph, each rail profile is linearized in a new coordinate S representing the length over the rail profile, as shown in Fig. 8. The coordinate S starts at zero at the profile field edge.

Four scenarios were simulated: tangent track with new rails, curved track with new rails, tangent track with worn rails, and curved track with worn rails. For each scenario, the contact of ten unique wheelsets were evaluated. Therefore, each pummelling analysis represents the summation of ten distinct contact pressure distributions. The wheels and rail profiles were obtained from the measurement of actual wheels and rails, the same used by Higa, Kina and Gay Neto [8] (Fig. 9 and Fig. 10). It includes wheel profiles with different characteristics, including thin flange, hollow, false flange, and no defects.

This study uses a section of a Brazilian heavy haul railway that runs 905 km from two state capitals in the country, Belo Horizonte and Vitória. The line has a metric gauge and mixed traffic includes both passenger and freight trains. Iron-ore is the main product transported.

For both SIMPACK® and VAMPIRE® simulations, tangent and curved track are evaluated in a single simulation. Thus, 20 simulations were performed in each software to evaluate all scenarios. The wagon travels at a constant speed of 65 km/h (18.05 m/s) in a track comprising of a tangent section with 150 m, a transition spiral for entry into the curve with 61.7 m, a curved section to the left with 195.6 m, a transition with 61.7 m and a final tangent section of 150 m; totaling 619 m traveled (Fig. 11). The track gauge is 1.0 m with rail cant of 1:40. At the curved section, the radius is 371.6 m and the superelevation is 57.2 mm. The total mass of the loaded wagon is 110,000 kg and the back-to-back distance between the wheels is 0.915 m.

For these simulations, the pummeling analyses were carried out with the contact data extracted from the front wheelset at the end of the first tangent section and the end of the curved section. Therefore, it represents the steady state of each section. Since both SIMPACK® and VAMPIRE® do not provide the contact pressure distribution as an output, such distributions were admitted as following the Hertz Contact Theory [22], i.e., a semi-elliptical distribution (Fig. 12). After the dynamic simulation, maximum contact pressure, the semi-axes of the ellipse and position of the contact on the rail were exported to MATLAB®, and the contact pressure distribution was calculated according to Eq. (10). In this equation, p_0 is the maximum contact pressure and b represents the semi-axis of the contact ellipse in the transverse direction of the track. P is the contact load.

$$p(s) = p_0 \sqrt{1 - \left(\frac{s}{b}\right)^2}$$

10

$$p_0 = \frac{3P}{2\pi ab}$$

11

For the quasi-static model, each scenario is simulated individually and 40 simulation were performed to evaluate all scenarios. The track and wagon parameters were the same as described for the multibody simulations.

3 RESULTS AND DISCUSSIONS

Figure 13 shows the pummelling plots (summed contact pressure distributions for all the simulations at a given condition), for new and worn rails on the tangent section comparing the quasi-static model (GIRAFFE), SIMPACK® and VAMPIRE®. At the corner of each plot, the rail profile and its coordinate S are presented as reference. For new rails (Fig. 13a and b), contact occurs on the top of the head for all models. In the left rail, for the SIMPACK® data (Fig. 13a), it is possible to see a contact in the outer shoulder, near 40 mm. This contact occurs due to the false flange. Preliminary studies looking for the reasons of this false flange showed that, for wheel profiles with severe hollow tread, SIMPACK® tends to fit one of the wheels with the rail while the other wheel stays in contact with the false flange (Fig. 14). The left rail presented a difference in the magnitude of the pressure between the models, while the right rail (Fig. 13b) presented a good agreement for all models. For worn rails (Fig. 13c and d) the pressure distribution is slightly broader and lower compared to the new rails. Considering the left rail of the tangent (Fig. 13c), the contact occurs on the top of the head for both dynamic models. However, GIRAFFE presents an additional contact locus in the inner side of the rail, different from the other two methods. Considering the right rail (Fig. 13d), a good agreement is observed with the contact at the top of the head.

VAMPIRE® and SIMPACK® results show good correlation in all cases. The observed differences are from how contact is calculated by each software. SIMPACK® uses the FASTSIM algorithm that presents an error for creep force estimation due to the parabolic traction bound compared with CONTACT algorithm, used to calculate the look-up table adopted by VAMPIRE® [24].

Figure 15a and b show the longitudinal and lateral creep forces, respectively. These graphics were developed for the same scenario presented in section 2.3, with the current wheel and rail profile as new. As can be seen in Fig. 15a, both models present the same longitudinal creep force in the tangent, before 200 m. In the curve, between 200 and 400 m, the left wheels present a good correlation while the right wheels present a significant difference of 70%. For the lateral creep force (Fig. 15b), as in the longitudinal, the results agree for the tangent section. In the curve, right wheel forces present a difference of 33% while for the left wheel forces the two models present approximately the same force magnitude, but with a different direction.

Figure 16 present the pummeling plot for new and worn rails on the curved section comparing the quasi-static model (GIRAFFE), SIMPACK® and VAMPIRE®. Considering the left new rail (Fig. 16a), two contact

loci appear for SIMPACK® and VAMPIRE® with a similar pressure magnitude, on the top of the head and on the outer shoulder of the rail. However, GIRAFFE presents only one contact locus in the top of the head. For the right new rail (Fig. 16b), VAMPIRE®, SIMPACK® and GIRAFFE present similar contact loci, with two contacts, on the top and inner shoulder. Considering the left worn rail (Fig. 16c), two contact loci appear, on the top of the head and the outer shoulder of the rail for SIMPACK® and VAMPIRE®, with a difference in the magnitude, while GIRAFFE presents a contact locus in the inner shoulder instead of the outer shoulder. For the right worn rail (Fig. 16d), as in the left, VAMPIRE® and SIMPACK® present similar contact loci with different pressure magnitudes, though GIRAFFE presents significant differences in both distribution and magnitude.

The influence of the geometric profile of the rail on the wheel/rail contact intensity and distribution is clear from Fig. 13 and Fig. 16. For example, in Fig. 16d the accumulated pressure distribution is broader than the distribution seen in Fig. 16b, since the high worn rail has a more conformal contact with this population of wheels. This also leads a 191% reduction in the peak pressure values. However, Fig. 16c shows higher values of accumulated pressure and narrower distribution than Fig. 16a for the low worn rail, for its flattened head is less conformal with the wheels' profiles. This result underlines the importance of the geometric profile on the wheel/rail contact.

As shown in Fig. 13, GIRAFFE's quasi-static model for the tangent section correlates well with the results obtained by dynamic simulations. However, Fig. 16 shows that GIRAFFE quasi-static model for the curved section presents more differences when compared to the dynamic models, mostly on the worn right rail (high). For the curved section in the GIRAFFE model, in addition to the gravitational force, a horizontal force is applied pointing to the right side (since the curve is to the left), which represents the centrifugal force of the related curve. However, in its present version, the quasi-static model does not include creep forces, which are considered in dynamic simulations. As shown by Sá et al. [25], the creep forces may contribute to the expected lateral positioning of the wheelsets. Since these are not currently considered in GIRAFFE model, it seems to be an important improvement for further research. Moreover, contact pressure results may differ for distinct tools when using distinct techniques, such as Hertzian, semi-Hertzian or other approaches. Even with such criticizing, and given the simplifications made, it seems that such a quasi-static approach can be useful for a first and fast assessment for wheel-rail contact loci, being convenient for diagnosing railway contact scenarios.

The total simulation time reduced from 475 seconds in Vampire (533 s in SIMPACK) to 126 s in GIRAFFE, a reduction of at least 73.4%. In the present work, only ten wheelsets were evaluated, however, for an effective pummeling analysis, which needs a large number of wheelsets, generally thousands, reducing computational cost becomes even more important.

4 CONCLUSIONS

In this work, we compared a quasi-static simplified model with two dynamic models from commercial software to evaluating pummelling analyses for the wheel-rail interaction. The quasi-static is solved

using the GIRAFFE program. SIMPACK® and VAMPIRE® multibody dynamics simulation programs are used to simulate the full dynamics of a railway wagon on a track layout. Heavy haul railway track parameters and vehicle loads are taken into account in the simulations. The results showed that the quasi-static model has a very good correlation with the dynamic models for the tangent conditions. For the curves, some differences were observed in the distribution of contact pressures. However, even with that, it seems that such a quasi-static approach can be useful as a first and fast assessment for wheel-rail contact loci, currently with some known limitations. Quasi-static simulations were 73.4% faster than multibody simulations. Besides, after further developments, the approach can be very useful for time consuming analysis, which requires many simulations.

The comparison between the dynamic models also showed distinct results due to the difference in how the contact is calculated. The results demonstrated the importance of the geometric profile to a more accurate representation of the contact.

The improvement of the quasi-static models, particularly in curve scenarios, claims the inclusion of the creep forces. This insertion will contribute to the more precise localization of the steady-state lateral average position of wheelsets. This subject will be addressed in future work.

Declarations

Author Contribution

P.A.P. Pacheco and T.L. Sá developed the models and wrote the first version of the main manuscript. P.A.P. Pacheco and P.G. Ramos developed the dynamic models and run the simulations; T.L. Sá and A. Gay Neto developed the quasi-static modelling; G.F.M. Santos and P.A.P. Pacheco developed the models and analyzed the contact region for dynamic simulation; A.A. Santos and A. Gay Neto defined the objectives and methodology for the research. All authors reviewed the manuscript. A.A. Santos, G.F.M. Santos, and A. Gay Neto are the project managers for this research in their own institutions.

ACKNOWLEDGMENTS

This project is grateful for the support of Vale S.A. through the Wheel-Rail and Wagons Chairs and the CNPq (National Council for Scientific and Technological Development) under grants 304321/2021-4 and 315304/2018-9.

References

1. L. Huang, Z. Li, L. Li and Q. An., "Methods to calculate accurate wheel/rail contact positions and static contact stress levels," Proc IMechE Part F: J Rail and Rapid Transit, vol. 230, pp. 138–150, 2016.

2. E. Magel and J. Kalousek, "The application of contact mechanics to rail profile design and rail grinding," *Wear*, vol. 253, pp. 308–316, 2002.
3. S. Bruni, J. P. Meijaard, G. Rill and A. L. Schwab, "State-of-the-art and challenges of railway and road vehicle dynamics with multibody dynamics approaches," Multibody System Dynamics, vol. 49, pp. 1–32, 2020.
4. J. C. Pombo and J. A. Ambrósio, "Application of a wheel–rail contact model to railway dynamics in small radius curved tracks," Multibody Syst Dyn, vol. 19, pp. 91–114, 2008.
5. E. Meli and A. Ridolfi, "An innovative wheel–rail contact model for railway vehicles under degraded adhesion conditions," Multibody Syst Dyn, vol. 33, pp. 285–313, 2015.
6. X. Yu, J. F. Aceituno, E. Kurvinen, M. K. Matikainen, P. Korkealaakso, A. Rouvinen, D. Jiang, J. L. Escalona and A. Mikkola, "Comparison of numerical and computational aspects between two constraint-based contact methods in the description of wheel/rail contacts," Multibody System Dynamics, vol. 54, pp. 303–344, 2022.
7. W. Ebersöhn, M. Trosino, E. Magel and M. El-Sibaie, "Managing wheel/rail performance on Amtrak's Northeast corridor," in *AREMA*, Washington, DC, 2002.
8. D. N. Higa, E. J. Kina and A. G. Neto, "Wheelset rail mechanical model for a steady-state dynamic condition and prediction of rolling contact fatigue locci," Vehicle System Dynamics, vol. 60:1, pp. 281–308, 2022.
9. E. A. Lima, L. B. Baruffaldi, J. L. B. Manetti, T. S. Martins and A. A. Santos, "Effect of truck shear pads on the dynamic behaviour of heavy haul railway cars," Vehicle System Dynamics, vol. 60, no. 4, pp. 1188–1208, 2022.
10. J. J. Kalker, "On the Rolling Contact of Two Elastic Bodies in the Presence of Dry Friction [Doctoral]," Technische Hogeschool, 1967.
11. J. J. Kalker, "Wheel-rail rolling contact theory," Wear, 1991.
12. J. J. Kalker, "A Fast Algorithm for the Simplified Theory of Rolling Contact," Vehicle System Dynamics, vol. 11(1), pp. 1–13, 1982.
13. S. Hossein-Nia, M. S. Sichani, S. Stichel and C. Casanueva, "Wheel life prediction model – an alternative to the FASTSIM algorithm for RCF," Vehicle System Dynamics, vol. 56(7), pp. 1051–1071, 2018.
14. F. C. Santos, "Análise do contato roda-trilho e suas influência na vida em serviço de rodas ferroviárias," *Master degree thesis*, 2000.
15. SIMPACK, "FASTSIM," in *Simpack User Assistance*, Dassault Systèmes Simulia Corp., 2022.
16. J. J. Kalker, Three-dlmensional elastic bodles in rolling contact, 1 ed., vol. 2, Springer Dordrecht, 1990, pp. XXVI, 314.
17. F. M. H. Marques, B. Liu, J. Pombo, P. Flores, J. Ambrósio, J. Piotrowski and S. Bruni, "On the generation of enhanced lookup tables for wheel-rail contact models," Wear, Vols. 434–435, 2019.
18. VAMPIRE, "Wheel Rail Creep Laws," in *Vampire help manual*, SNC-Lavalin, 2020, pp. 757–791.

19. A. Gay Neto, P. M. Pimenta and P. Wriggers, "A master-surface to master-surface formulation for beam to beam contact. Part I: frictionless interaction," Computer Methods in Applied Mechanics and Engineering, vol. 303, pp. 400–429, 2016.
20. L. Silva and A. Gay Neto, "Geometry reconstruction based on arc splines with application to wheel-rail contact simulation," *Engineering Computations*, Vols. ahead-of-print, no. ahead-of-print, 2023.
21. A. G. Neto, "GIRAFFE Platform," 2022. [Online]. Available: http://sites.poli.usp.br/p/alfredo.gay/#giraffe-section. [Accessed 12 December 2022].
22. K. L. JOHNSON, Contact Mechanics, Cambridge: Cambridge University Press, 1985.
23. Q. J. Wang and D. Zhu, "Hertz Theory: Contact of Ellipsoidal Surfaces," Encyclopedia of Tribology, 2013.
24. M. S. Sichani, R. Enblom and M. Berg, "An alternative to FASTSIM for tangential solution of the wheel–rail contact," Vehicle System Dynamics, vol. 54:6, pp. 748–764, 2016.
25. T. L. Sá, P. G. Ramos, P. A. P. Pacheco, M. Viana, G. F. M. Santos, A. A. S. Junior and A. G. Neto, "Comparison between dynamic and quasi-static model to evaluate wheel-rail contacts," in *In: V Simpósio de Engenharia Ferroviária*, Campinas, 2022.

Figures

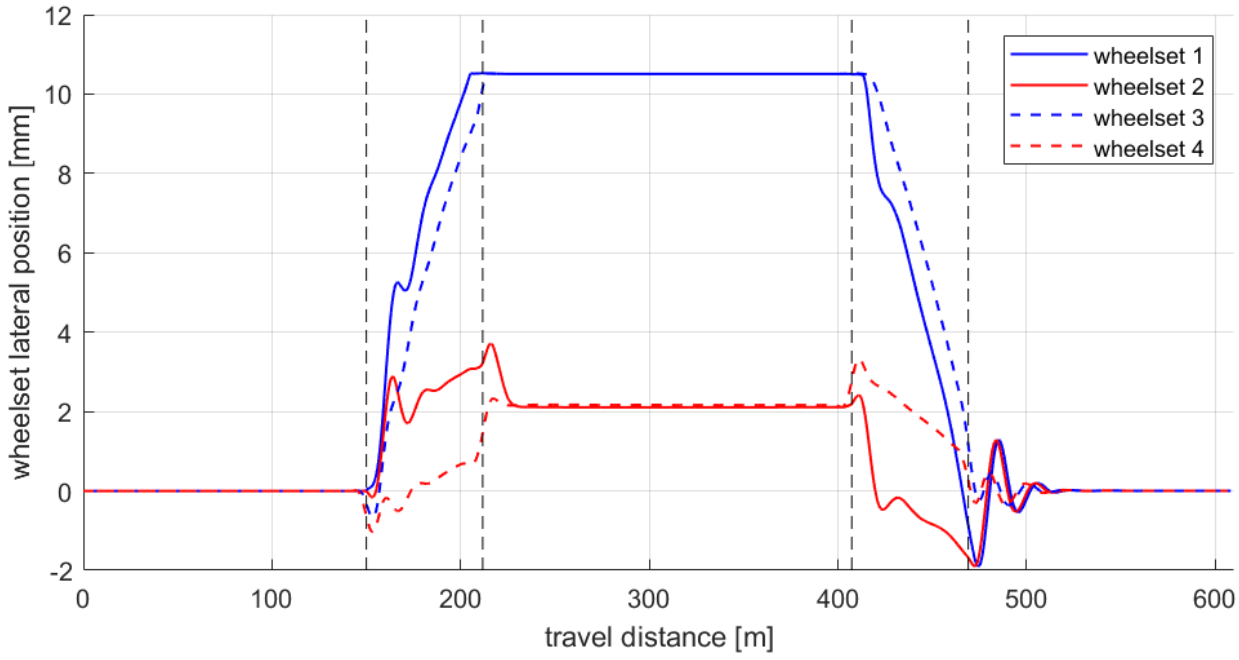

Figure 1

Wheelset steady-states on a multibody dynamic simulation of a complete wagon.

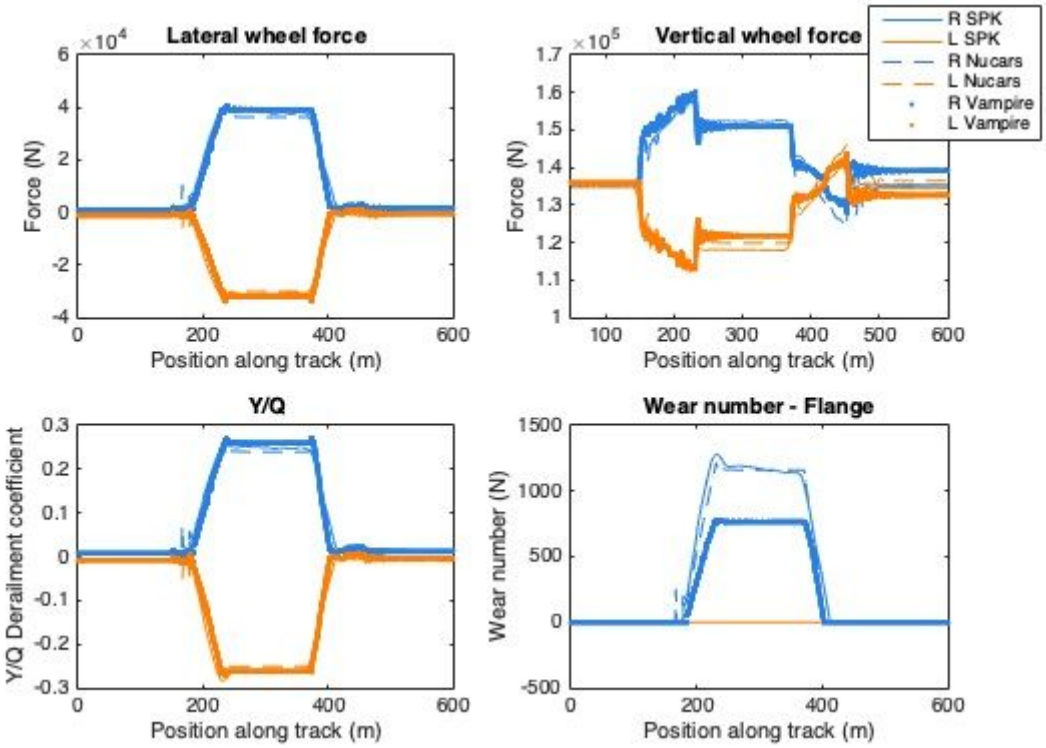

Figure 2

Dynamic model validation. L for left, R for right, and SPK for SIMPACK.

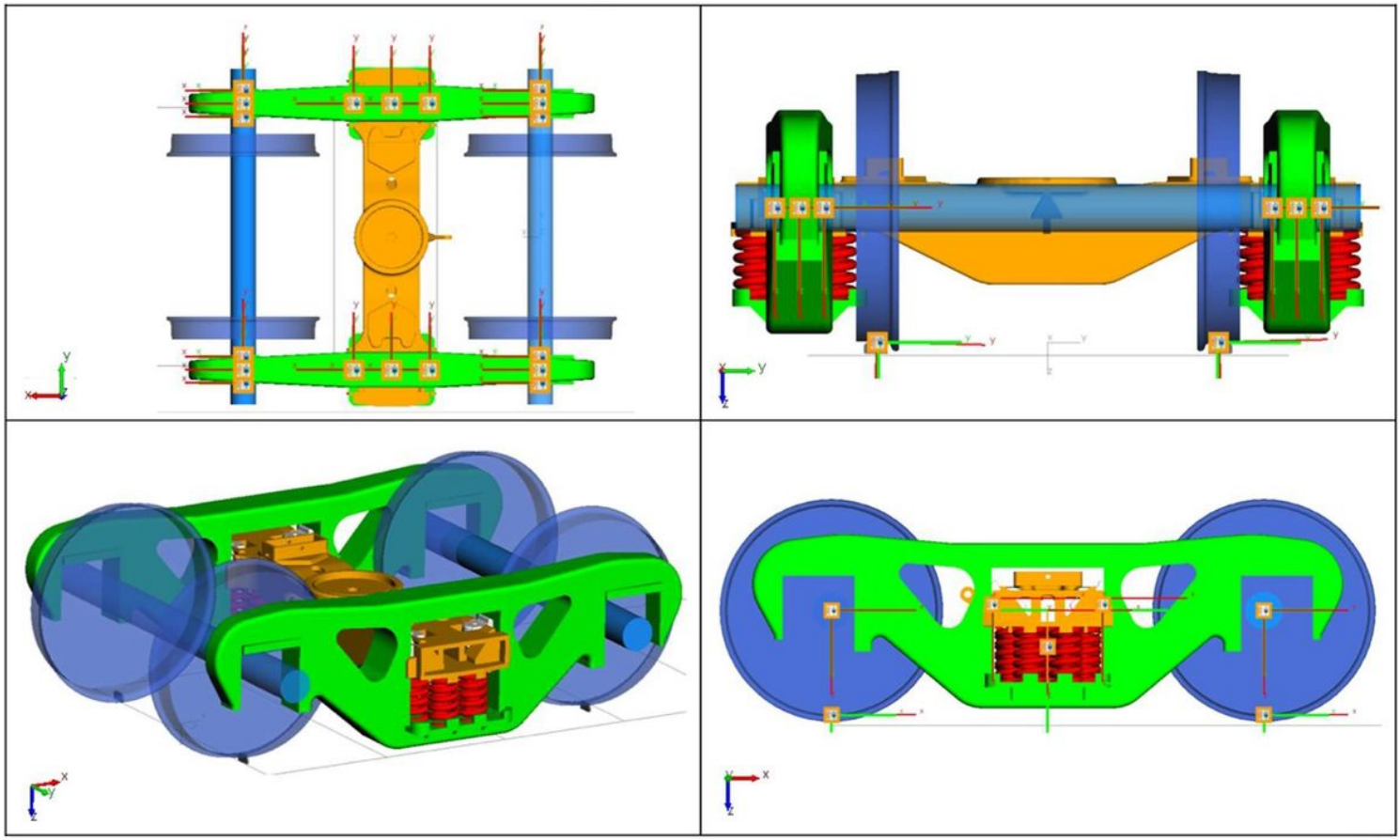

Figure 3

Bogie model of the GDE – Ride Control Wagon in SIMPACK®.

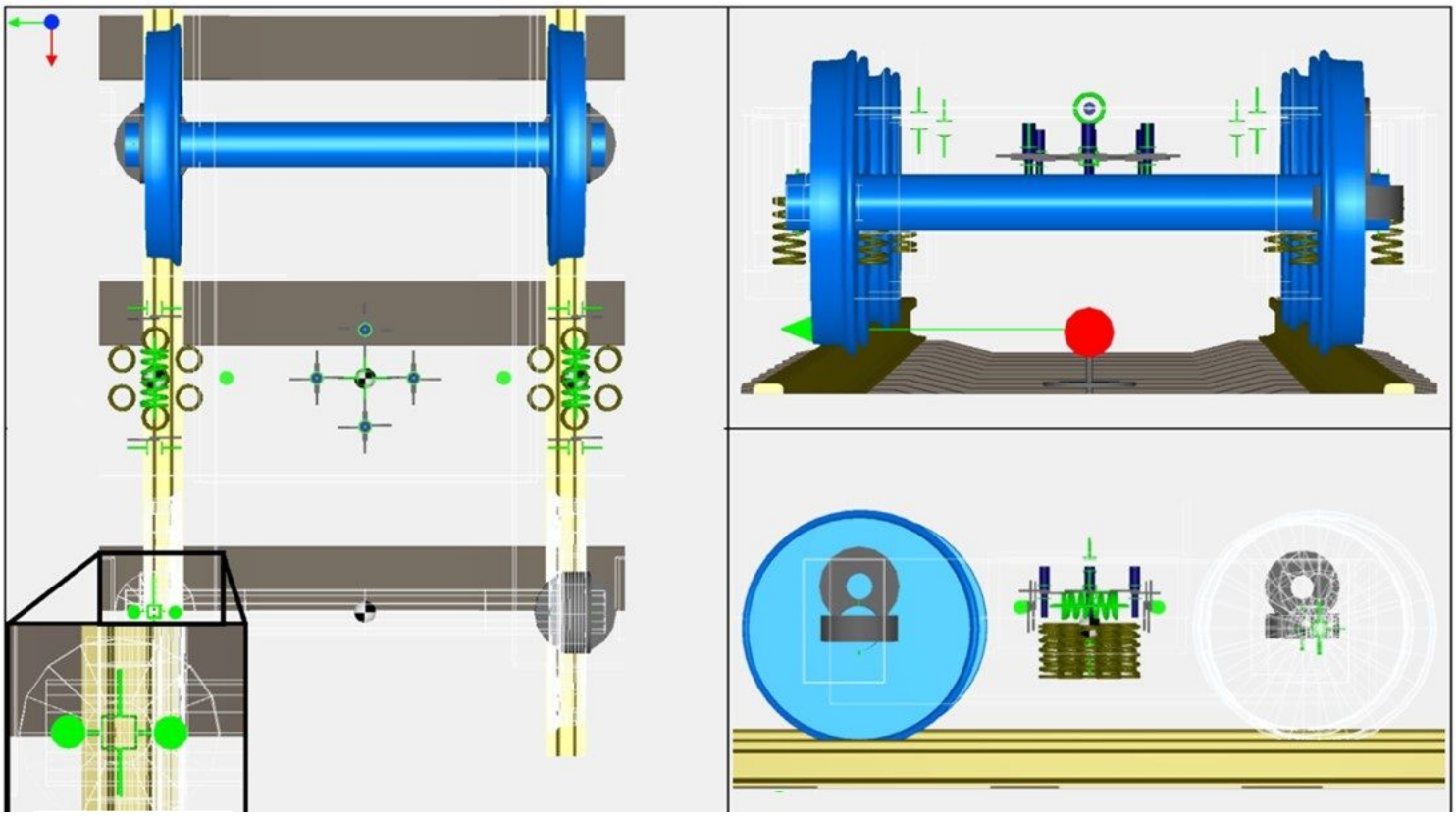

Figure 4

Bogie model of the GDE – Ride Control Wagon in VAMPIRE®.

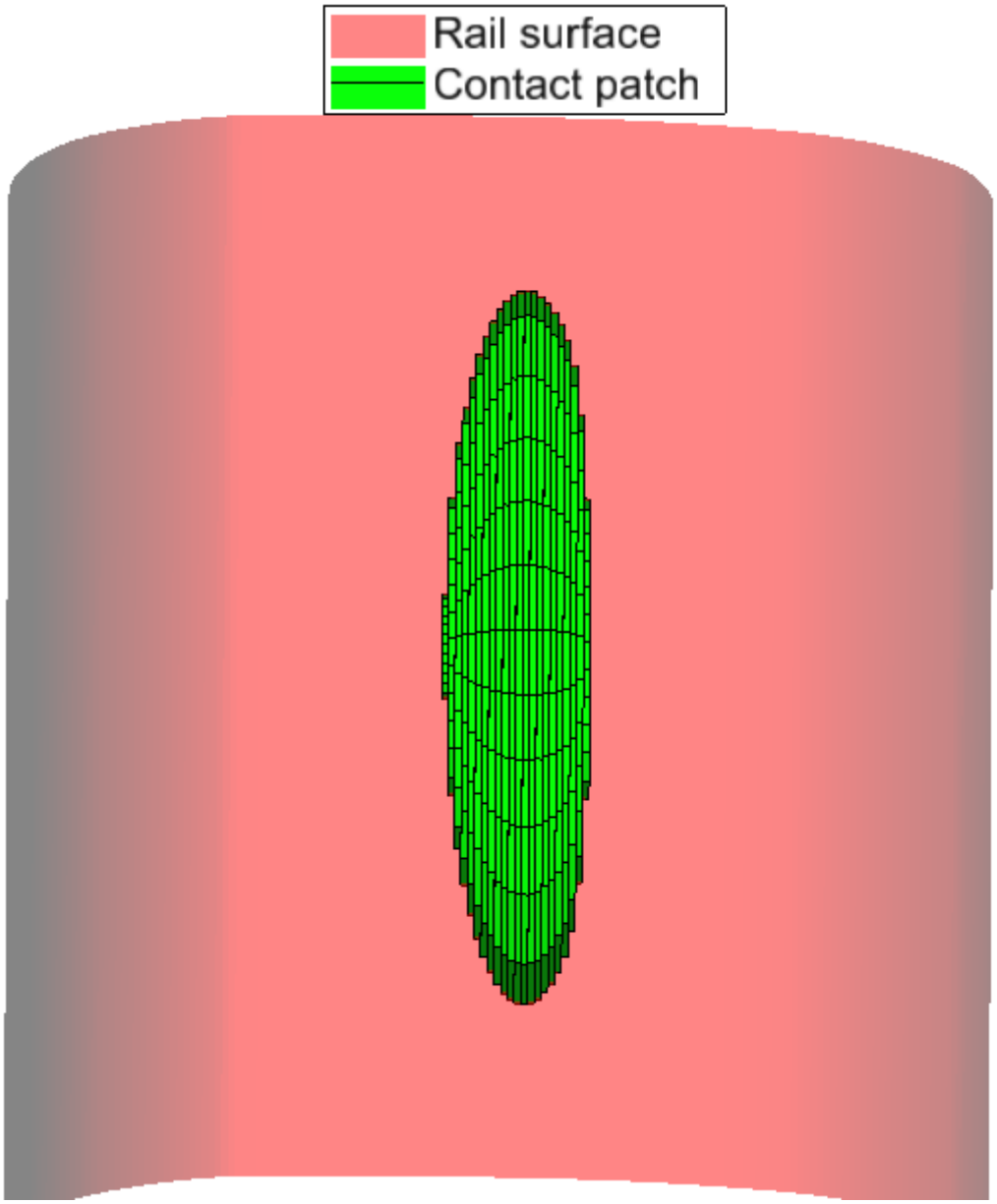

Figure 5

FASTSIM discretisation of the contact patch.

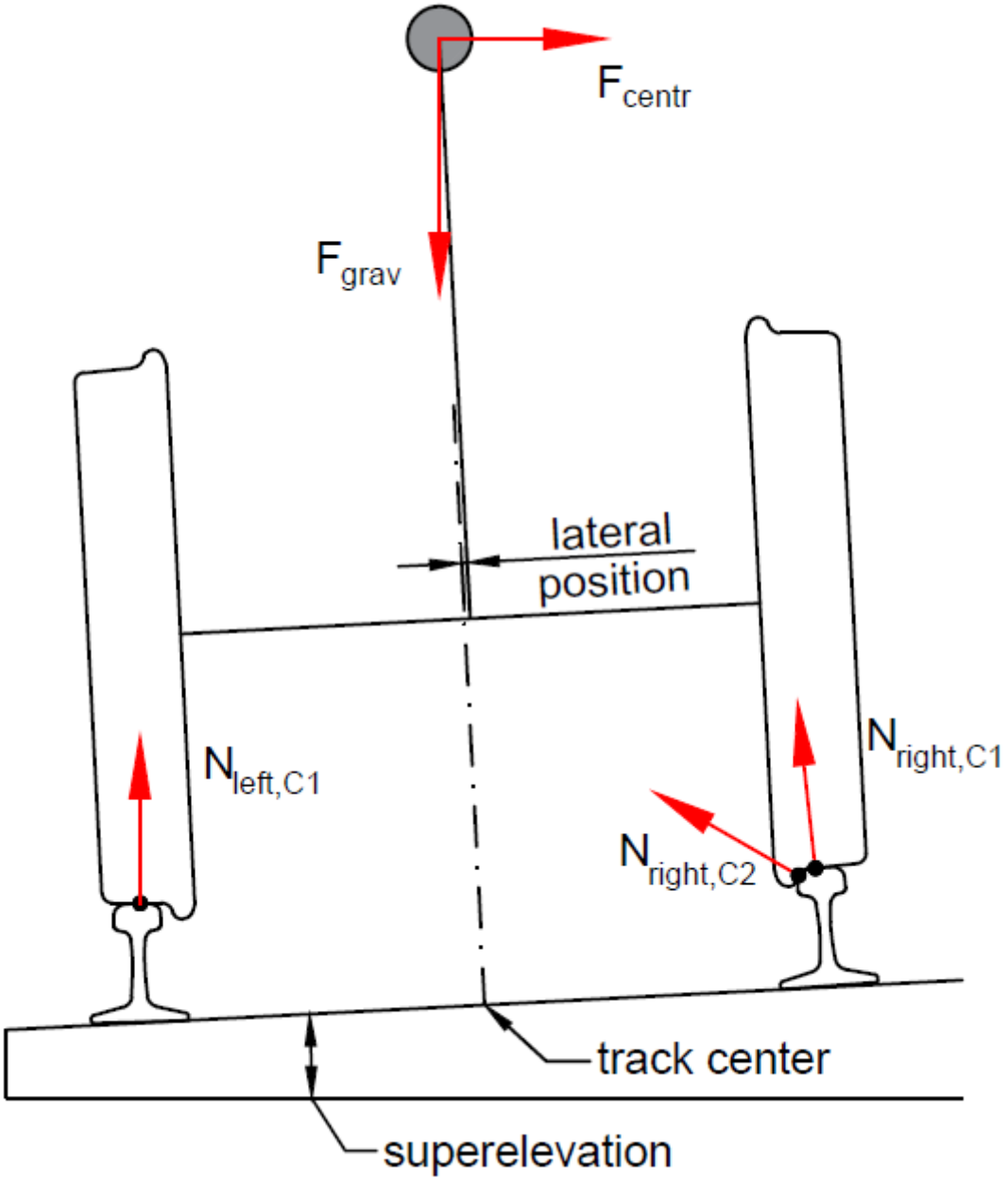

Figure 6

Equilibrium of forces at the quasi-static model (adpated from [8])

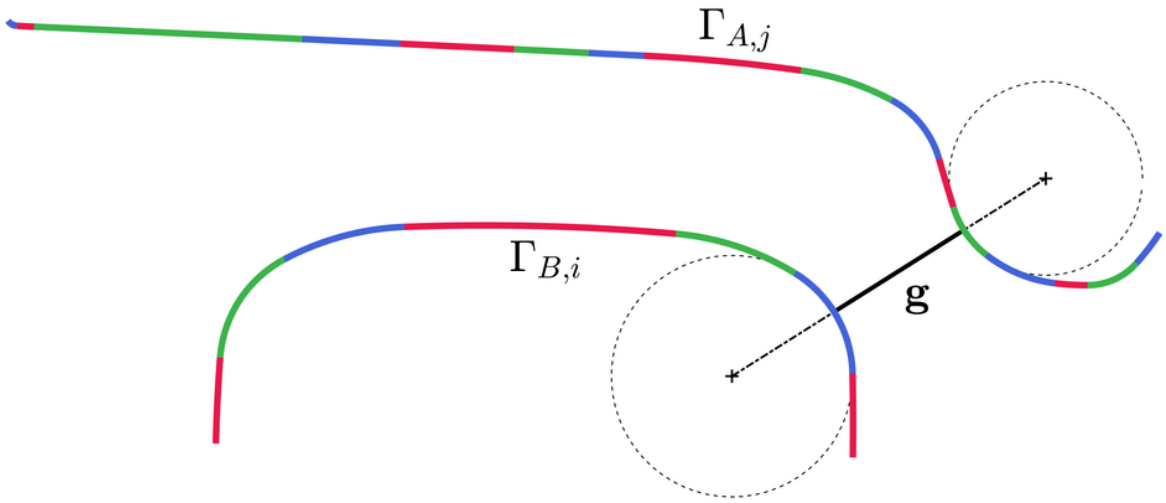

Figure 7

Set of arcs composing the wheel and rail geometric profiles (adapted from [8])

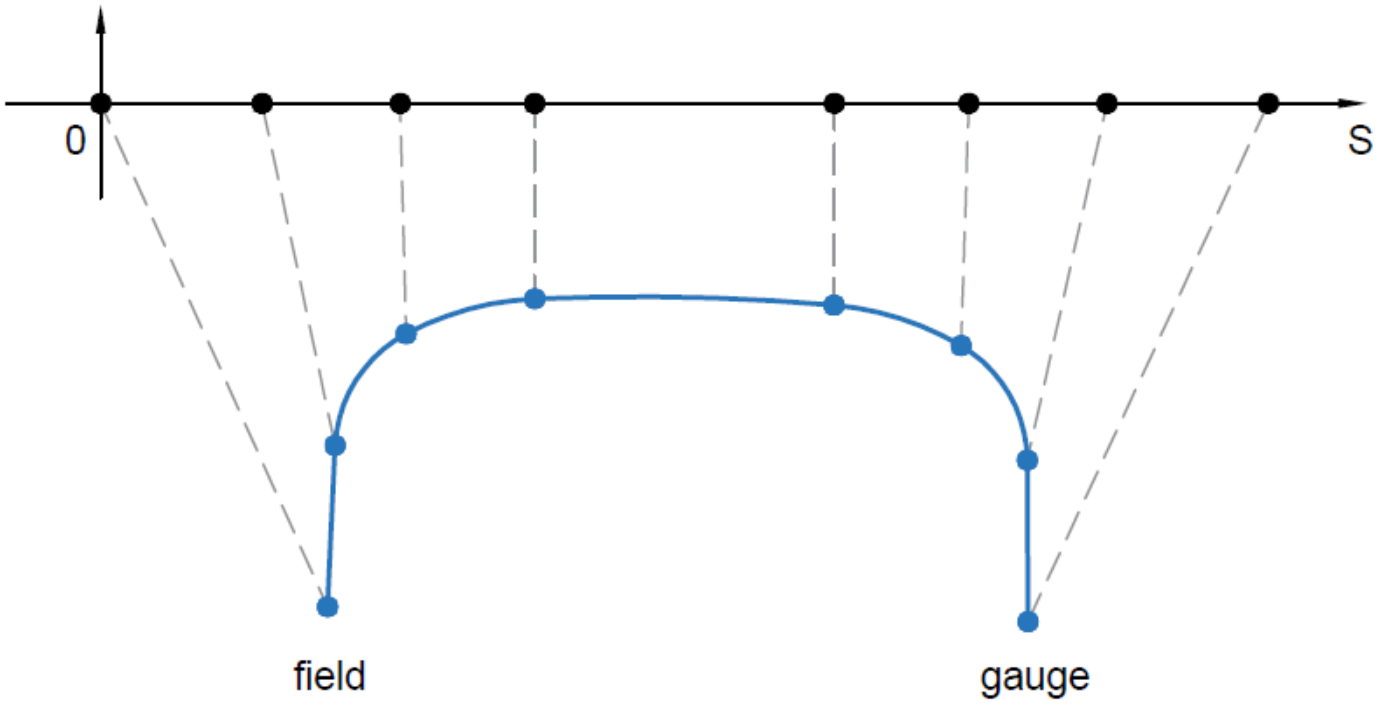

Figure 8

Rail profile linearization (adapted from [8]).

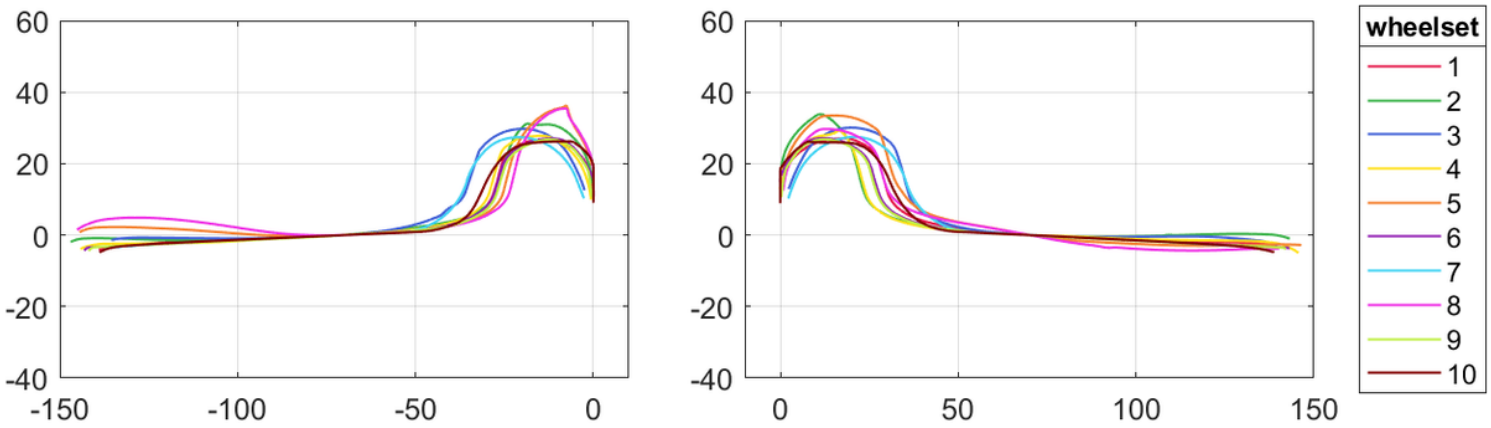

Figure 9

Left and right wheel profiles of each wheelset. Dimensions in mm.

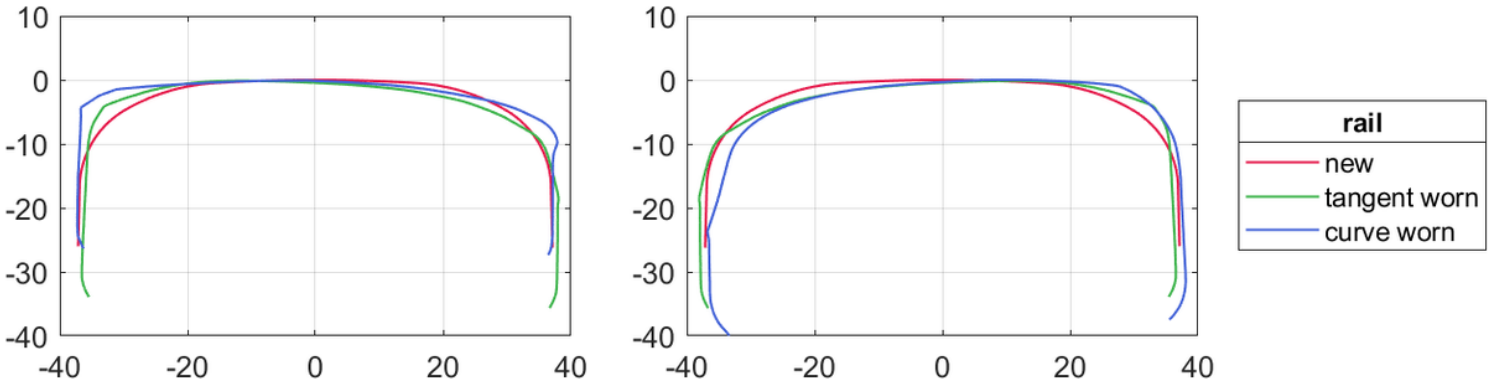

Figure 10

Left and right rail profiles. Dimensions in mm.

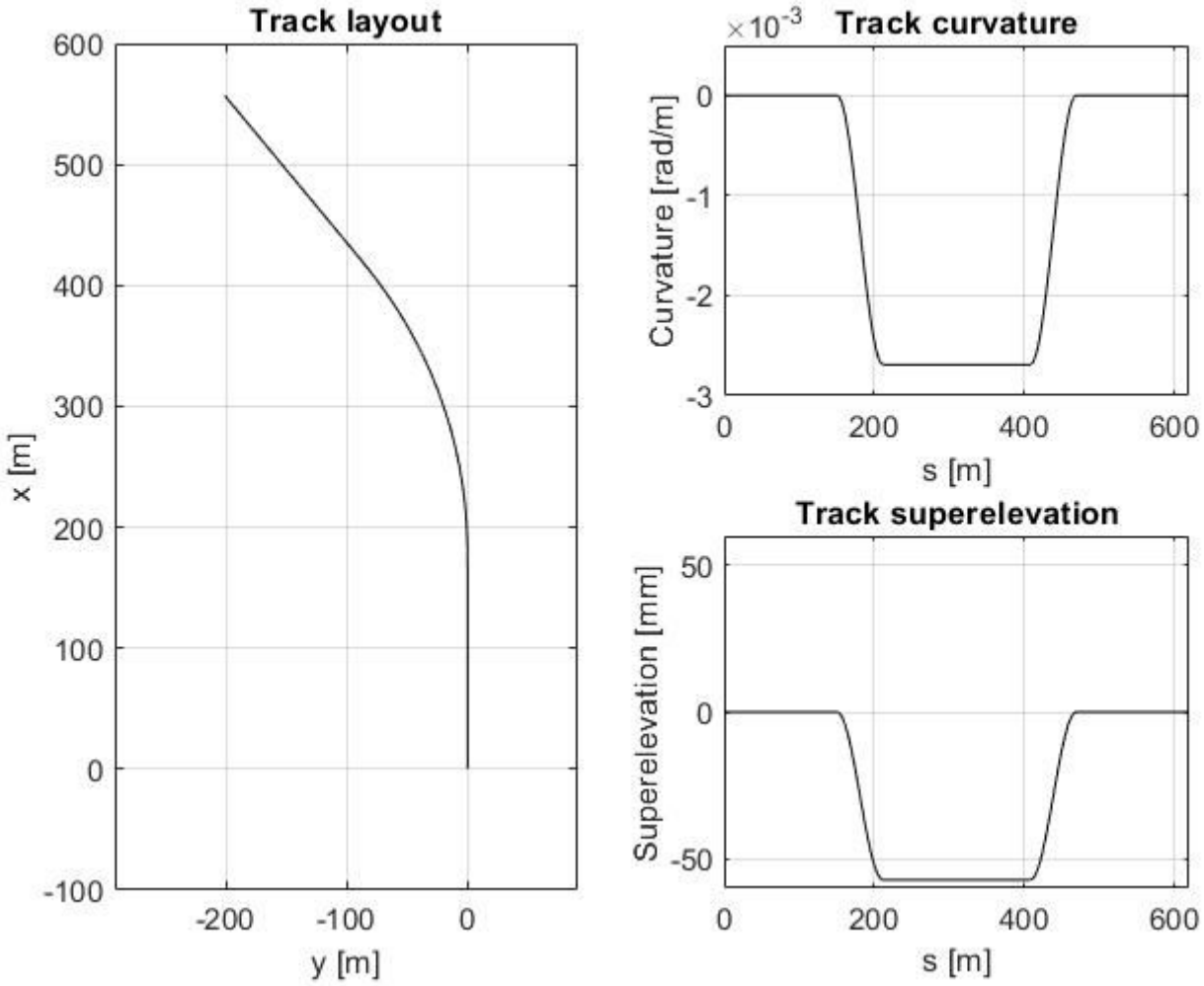

Figure 11

Track layout (x-y plot), curvature, and superelevation.

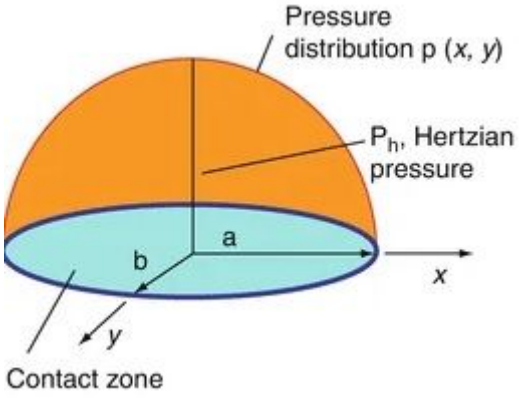

Figure 12

Pressure distribution in the elliptical contact [23].

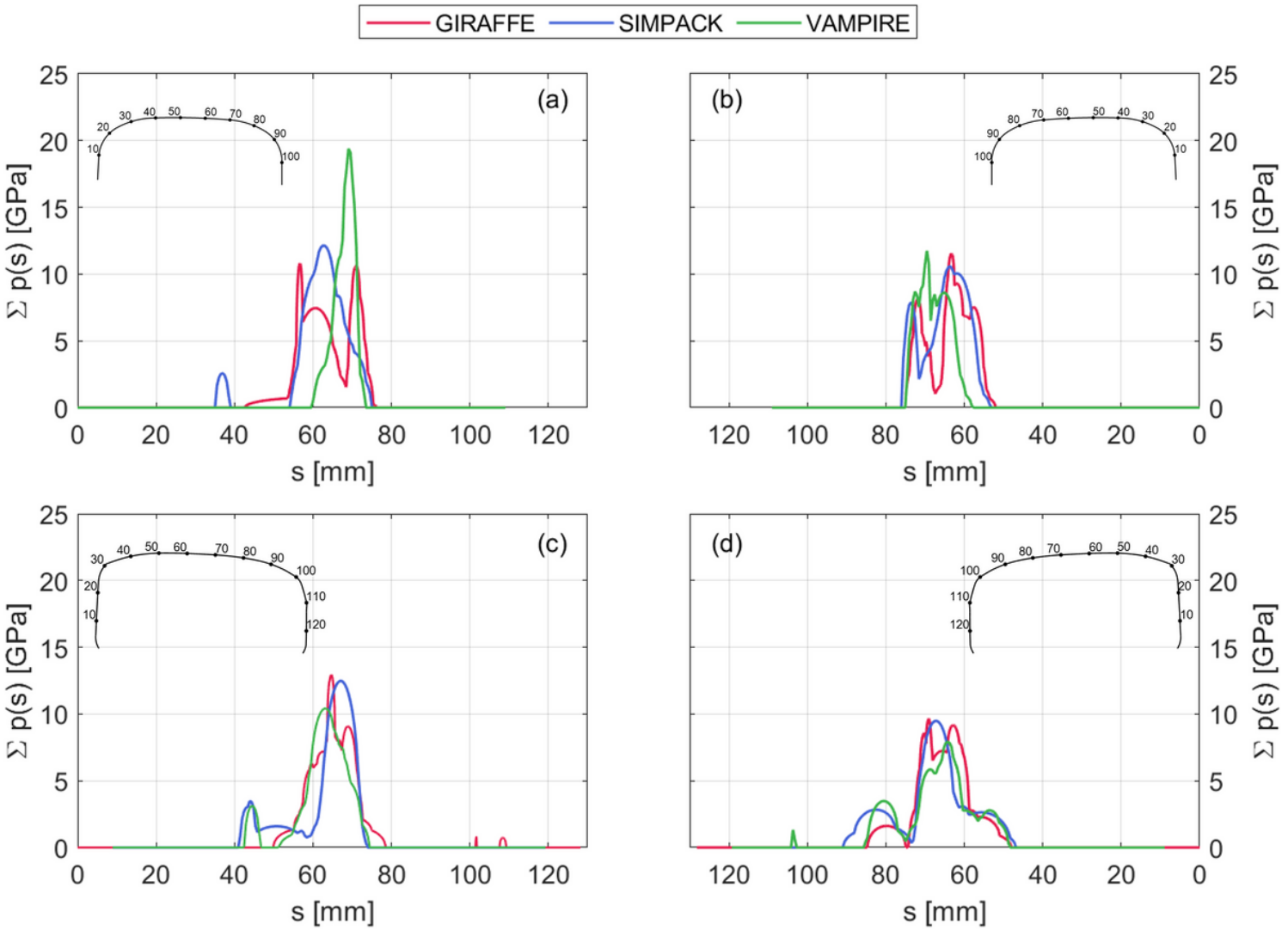

Figure 13

Contact pressure summation for tangent track: (a) new rail left; (b) new rail right; (c) worn rail left; (d) worn rail right.

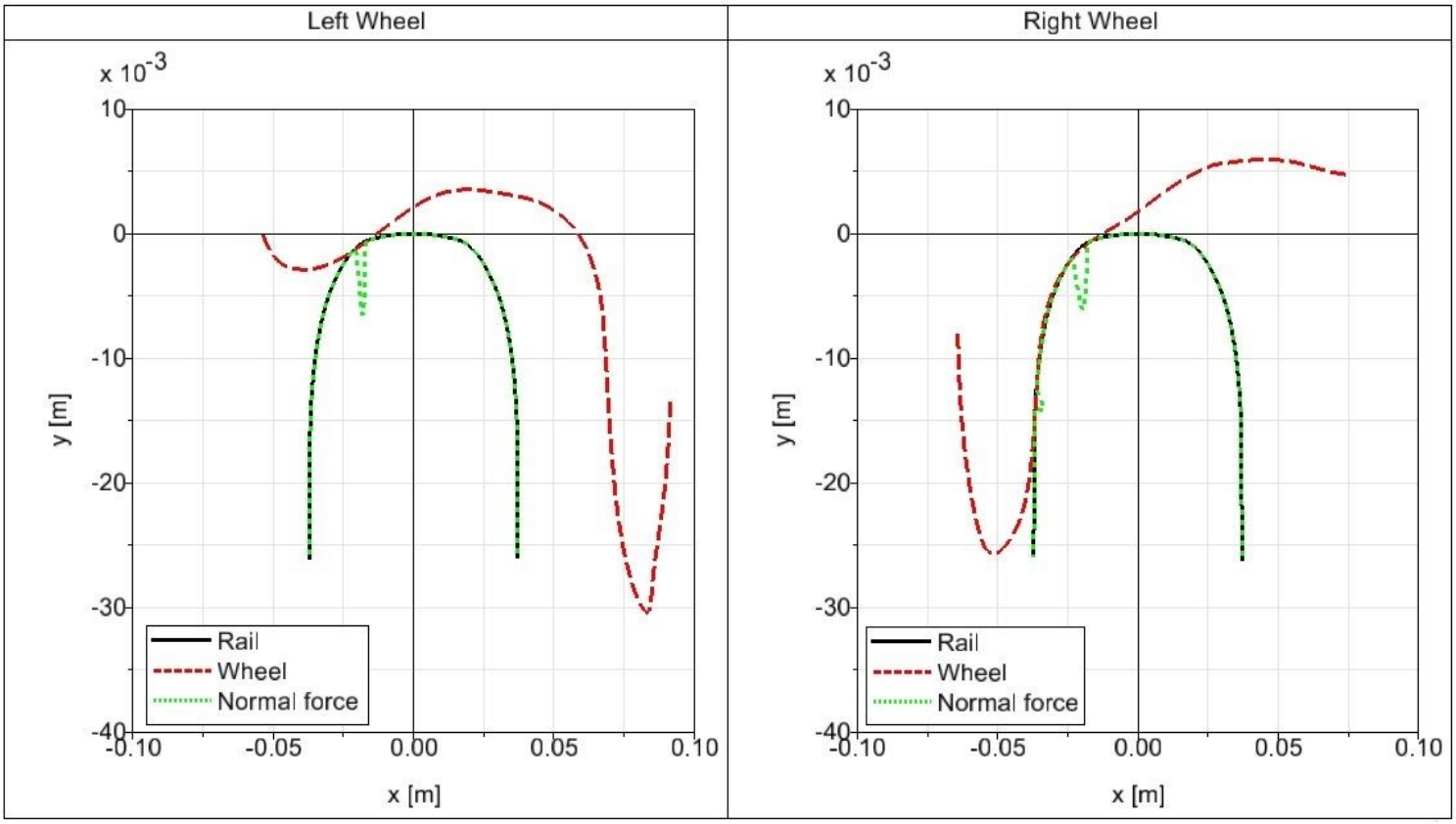

Figure 14

Wheel/Rail contact in SIMPACK®.

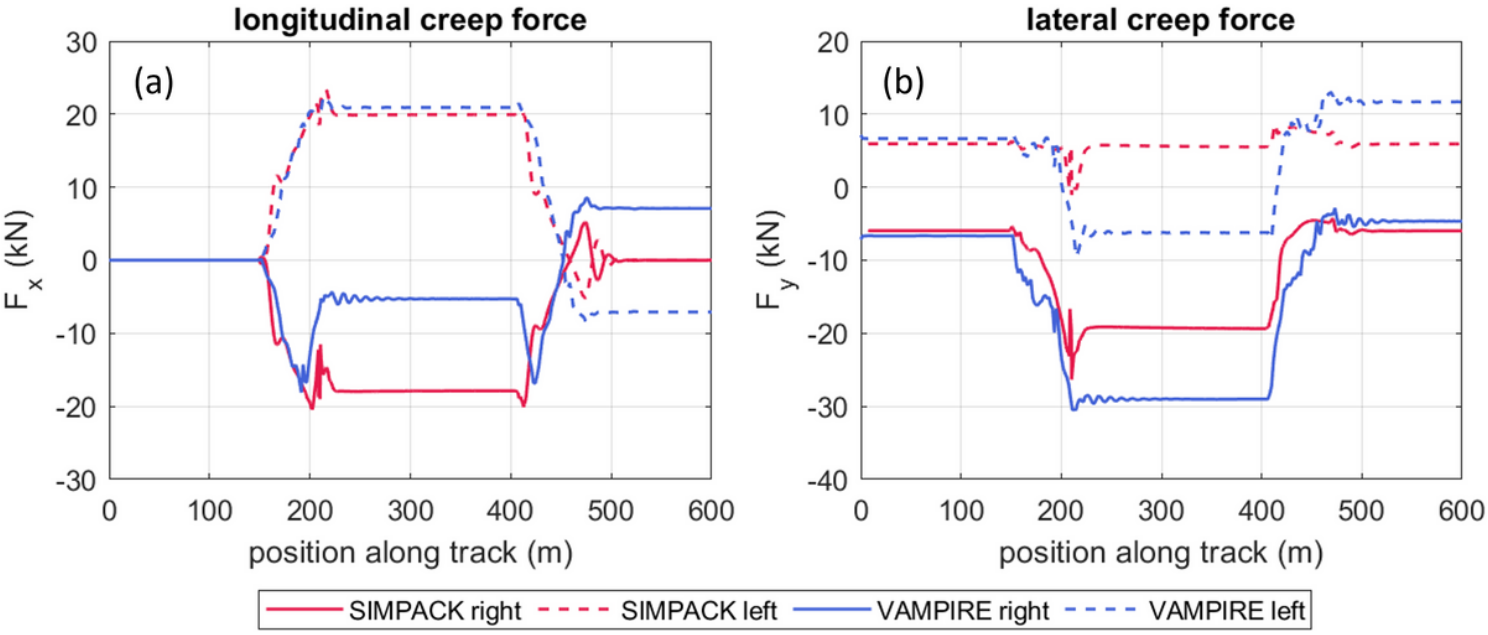

Figure 15

Comparison of longitudinal and lateral creep forces for SIMPACK® and VAMPIRE®.

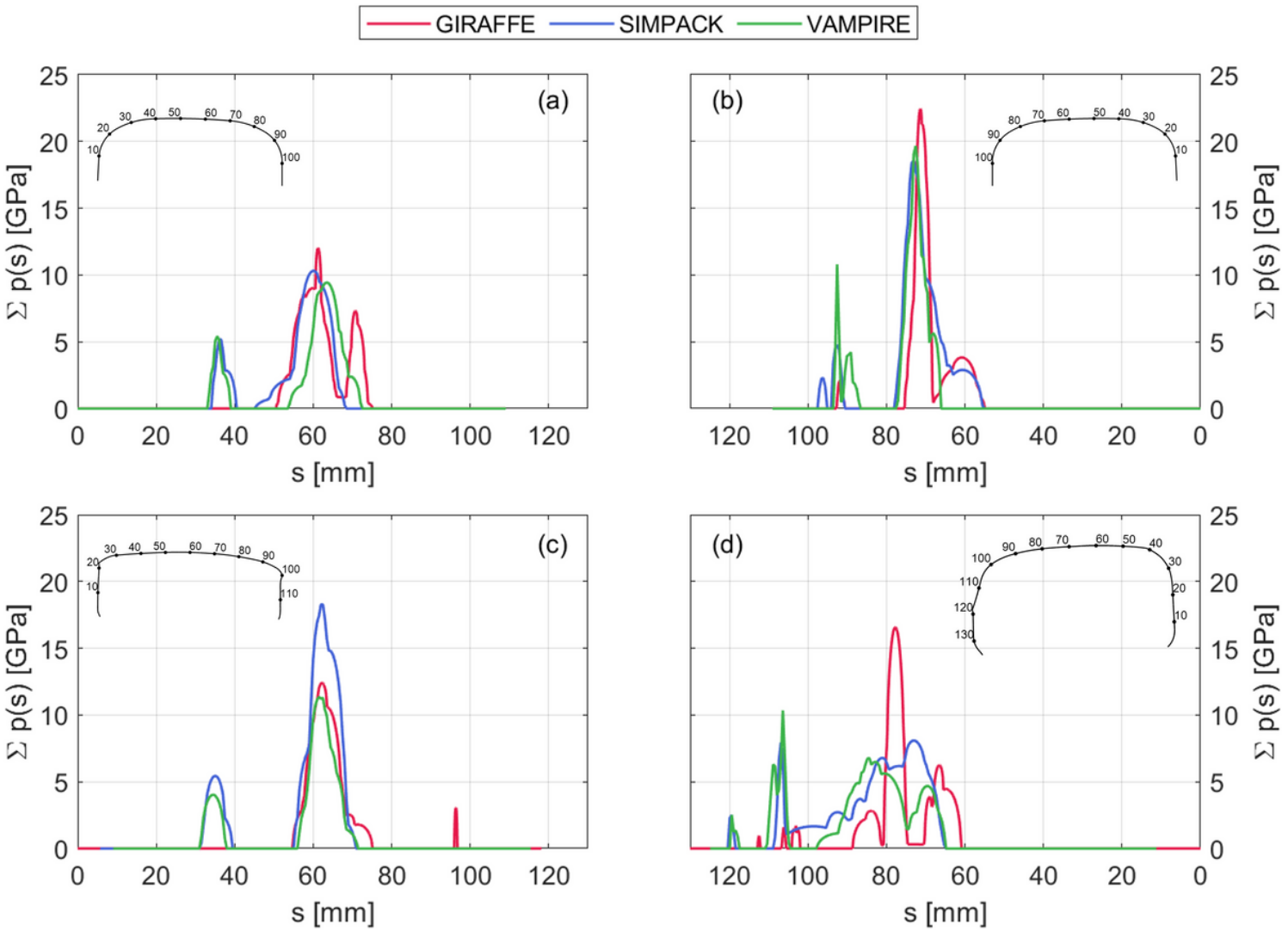

Figure 16

Contact pressure summation for curved track: (a) new rail left (low); (b) new rail right (high); (c) worn rail left (low); (d) worn rail right (high).